Reduction of Dietrich-Ruina attractors to unimodal maps

S. Shkoller[1] and J.-B. Minster[2],*

[1]Center for Nonlinear Studies MS-B258, Los Alamos National Laboratory, Los Alamos, NM 87545
[2]Institute of Geophysics and Planetary Physics, University of California at San Diego, La Jolla, CA 92093-0225

Abstract. We present a geometric analysis of a quasi-static single degree of freedom elastic slider with a state and rate dependent friction law. In particular, we examine and characterize the regime of chaotic motions displayed by the Dietrich-Ruina model. We do so by numerically reducing the chaotic attractors to a family of unimodal maps and discuss why this suggests complex behavior in the dynamical system.

1 Introduction

In this note, we examine and classify the quasi-static *chaotic* motion of a single degree of freedom elastic system undergoing frictional slip. Our interest is in friction laws of the state and rate dependent type, wherein the constitutive law has a fading-memory functional dependence on velocity paths. The functional dependence can be well approximated by a nonlinear dependence on current rate of slip together with a number of internal state variables; for a fixed normal stress σ, the constitutive relations may be expressed as

$$
\begin{aligned}
\tau &= F(v, \theta_1, \theta_2, ...), \\
\dot{\theta}_1 &= G_1(v, \theta_1, \theta_2, ...), \\
\dot{\theta}_2 &= G_2(v, \theta_1, \theta_2, ...), \\
&\vdots
\end{aligned}
\tag{1}
$$

where τ is the shear force transmitted across the frictional surface, v is the current rate of slip or velocity, and where the state variables θ_i are intended to describe the changing features of the slipping surface. The functions F and G_i are, in general, phenomenologically derived, and chosen such that the state variables evolve toward a steady-state value.

Such friction laws have been studied extensively in the recent literature in the context of nonlinear sliders, with and without inertia, and with varying numbers of internal state variables. We refer the reader to Ruina (1983), Gu et al. (1984), Blanpied and Tullis (1986), Gu and Wong (1991),

Correspondence to: S. Shkoller

Gu and Wong (1994), Weeks (1993), and the references therein, for detailed studies of the generated dynamics as well as discussions regarding the effectiveness of such models for predicting and reproducing observations and experiments in rock mechanics.

Herein, we focus on the characterization of the chaotic motion produced by the simplest and perhaps most popular of the friction models from the general class of constitutive laws described in (1), the Dietrich-Ruina or D-R model. To the best of our knowledge, such a characterization has not previously been made, even though it is essential to those interested in the route taken by friction towards complex behavior.

In the absence of inertia, the simplest D-R model that allows us to investigate the chaotic regime of the dynamics is the two state variable model which we express for a constant normal stress σ by

$$
\begin{aligned}
\tau &= F(v, \theta_1, \theta_2) := \tau_* + \theta_1 + \theta_2 + a \log \tfrac{v}{v_*}, \\
\dot{\theta}_1 &= G_1(v, \theta_1, \theta_2) := -\tfrac{v}{L_1}\left(\theta_1 + b_1 \log \tfrac{v}{v_*}\right), \\
\dot{\theta}_2 &= G_2(v, \theta_1, \theta_2) := -\tfrac{v}{L_2}\left(\theta_2 + b_2 \log \tfrac{v}{v_*}\right), \\
\dot{\tau} &= k(v_0 - v)
\end{aligned}
\tag{2}
$$

where v_*, τ_*, a, b_1, b_2, L_1, and L_2 are constants which are determined from experimental fit, and in addition to the already defined variables, the elastic stiffness is denoted by k, and the given slider velocity by v_0.

As is discussed in great detail in Gu et al. (1984) and Blanpied and Tullis (1986), this model exhibits many of the important characteristics of the behavior observed in previous laboratory experiments on rocks. In particular, step increases in slip rates of steadily sliding surfaces lead to sudden increases in the frictional stress followed by exponential decay towards a substantially smaller value. The length parameters L_1 and L_2 in this model can be thought of as some representative decay slip distances for the relaxation process. Similarly, the internal state variable may be interpreted as resistive stress which define the internal state of the frictional surface. Herein, we study the qualitative behavior of (2) as

the spring stiffness k varies, and fix the other parameters to be $v_0 = .5$, $a = .33$, $b_1/a = 1.$, $b_2/a = .84$, $L_1 = 5.2$, $L_2 = .25$, $v_* = 1$, and $\tau_* = 0$. The description of how this data was obtained by a numerical fit of the experimental observations can be found in Ruina (1983), Gu et al. (1984), and Blanpied and Tullis (1986).

As with most highly nonlinear non-integrable dynamical systems, we must rely on computational schemes to provide insight on the behavior of our model. Although this issue has not been widely addressed in the geophysical literature, the point must be made that the solutions obtained numerically are not solutions of the actual dynamical system, but rather of its discretized counterpart. One may consult any book on numerical methods to convince oneself that an appropriately chosen computational algorithm can provide excellent approximations to the actual solution *for a finite time interval*; however, one must be very careful in making any inferences about the actual attracting sets of the dynamical system from those which are computed numerically, as this would require the numerical scheme to approximate the dynamics for infinite time intervals, and in general, this does not occur. In the rare instance that the numerically computed attracting set converges to the actual attracting set as the discretization size (or time step) tends to zero, we say that the family of numerically computed attractors is continuous. In general, however, the numerically computed attracting sets either converge to a set that strictly contains or is strictly contained in the actual attractor, but not both. The reader is referred to Jones and Shkoller (1997) for examples and further discussion of this phenomenon.

The main result of the work of Pliss and Sell (1991) states that hyperbolic attractors persist under numerical perturbation. The term hyperbolic simply means that the linearization of the dynamics along the attractor has eigenvalues whose imaginary parts are not equal to zero. By numerical perturbation, we mean that the discretized equations may be thought of as being a small perturbation of the actual equations in some appropriately chosen norm or measure, when the numerical scheme is a "nice" one. Our objective in understanding the route to chaos and the type of chaotic attractors that the simplest D-R model provides is accomplished by reducing the attracting set in the three-dimensional phase space to a simple family of unimodal maps defined on an interval in one-dimension. Although we do not a priori know how small our numerical discretization must be in order to know that the numerically computed attractors do indeed approximate the actual chaotic attractor, our numerical reduction to piecewise polynomial unimodal maps and their convergence to smooth unimodal maps in the limit of zero time step is very convincing evidence that we have captured the true chaotic motions of the nonlinear slider.

The paper is structured as follows. In Section 2, we re-express the D-R model in the form of a three-dimensional vector field and then provide a complete geometric analysis of the dynamics, from the regime of stable steady sliding, through the Hopf bifurcation, where the stable steady sliding solution bifurcates into unstable steady sliding along

with stable periodic motions. This is determined by a nonlinear analysis using center manifold and normal form techniques, and is quite straightforward since the phase space is only three-dimensional. In Section 3, we perform some Lyapunov exponent calculations to get some insight as to the critical elastic stiffness where stable periodic motion becomes chaotic, and we give some discussion concerning what we have learned from numerous numerical experiments. Finally, in Section 4, we use a Poincaré map to construct numerically our family of unimodal maps, and from this we discover the period doubling route to chaotic dynamics.

2 Analysis

We begin be rewriting the D-R model in (2) as an evolution equation for a single vector $x \in \mathbb{R}^3$ with the elastic stiffness k as a parameter. By defining the vector $x := (\tau, \theta_1, \theta_2)$ where τ, θ_1, and θ_2 are its components in the usual basis, equation (2) takes the form

$$\dot{x} = f(x, k), \ f \in C^\infty(\mathbb{R}^3 \times \mathbb{R}^1, \mathbb{R}^3),$$
$$f(x) = \left(k(v_0 - e^{d/a}), \frac{-e^{d/a}}{L_1}(x_2 + \frac{b_1 d}{a}), \frac{-e^{d/a}}{L_2}(x_3 + \frac{b_2 d}{a}) \right),$$
$$d = x_1 - x_2 - x_3,$$
(3)

where the rate of slip or velocity $v = e^{d/a}$, and the notation $C^\infty(\mathbb{R}^3 \times \mathbb{R}^1, \mathbb{R}^3)$ means we are considering smooth three-dimensional vector fields whose domain are the points in three-dimensional space and a scalar parameter.

We begin our nonlinear stability analysis by noting, as in Gu et al. (1984), that the fixed-point $\bar{x}$ where steady sliding occurs corresponds to

$$\bar{x} = (a - b_1 - b_2, -b_1, -b_2) \log(v_0).$$
(4)

A complete local stability analysis of this equilibrium point is made by linearizing or taking the first variation of equation (3) about the steady state solution $\bar{x}$:

$$\dot{z} = Df(x, k)z, \ z \in \mathbb{R}^3.$$

Figure 1 shows the eigenvalues of $Df(\bar{x}, k)$ as a function of k. For large positive k, all the eigenvalues of $Df(\bar{x}, k)$ have negative real part indicating that the fixed point $\bar{x}$ is stable; however, as k decreases to $k_{cr} = .1061$, the fixed point becomes non-hyperbolic meaning that the complex conjugate pair of eigenvalues have zero real part. For $k < k_{cr}$, the conjugate pair have positive real part and the fixed point is unstable. Thus, at $k = k_{cr}$, the orbit structure of the linearized vector field near $(\bar{x}, k_{cr})$ may reveal *little* or possibly *incorrect* information regarding the stability of the fixed point.

Corresponding to the conjugate pair of eigenvalues located on the imaginary axis when $k = k_{cr}$, are two generalized eigenvectors whose span defines what is called the center subspace. The remaining eigenvalue is strictly real and negative; associated to it is a single generalized eigenvector whose span is called the stable subspace. As we will discuss below, in a small enough neighborhood, of the fixed point $\bar{x}$ at
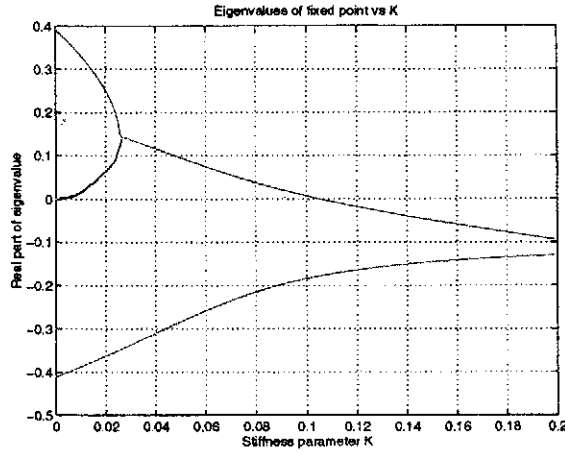
Fig. 1. Eigenvalues of the the dynamical system linearized about the fixed point as a function of the stiffness parameter k.

$k = k_{cr}$, say U, the dynamics are dissipative and this leads to the existence of a function defined on the center subspace whose graph is called the center manifold, and which all trajectories starting in U exponentially converge to. This is the essence of the theory of center manifolds and we refer the reader to Carr (1981) for a complete discussion as well as detailed proofs of this method. The main idea is that if we are ultimately interested in the nonlinear asymptotic behavior of our dynamical system near a bifurcation point, we can reduce our phase space from three to two dimensions by restricting the dynamics to the two dimensional center manifold, and hence significantly simplify our analysis.

We begin by moving $\bar{x}$ to the origin, and letting $\xi = x - \bar{x}$. The vector field becomes $\dot{\xi} = f(\bar{x} + \xi)$, $\xi \in \mathbb{R}^3$. A Taylor expansion about $\bar{x}$ then gives $\dot{\xi} = Df(\bar{x})\xi + F(\xi)$, $\xi \in \mathbb{R}^3$, where $F(\xi) = \mathcal{O}(|\xi|^2)$ and where we have suppressed explicit dependence on k. Through a linear conjugate transformation T, the linearized vector field can be written as

$$\begin{bmatrix} \dot{u} \\ \dot{w} \end{bmatrix} = \begin{bmatrix} A_s & 0 \\ 0 & A_c \end{bmatrix} \begin{bmatrix} u \\ w \end{bmatrix}, \ (u, w) \in \mathbb{R}^1 \times \mathbb{R}^2.$$

where A_s and A_c are the 1×1 and 2×2 matrices of generalized eigenvectors corresponding to the stable and center subspaces, and $(u, w) = T^{-1}x$. The dynamical system (3) can then be transformed to

$$\dot{u} = A_s u + F_s(u, w),$$
$$\dot{w} = A_c w + F_c(u, w),$$

where $F_s(u, w)$, and $F_c(u, w)$ are the first s and c components of $T^{-1}F(T(u, w))$. The center manifold theorem then asserts that there exists locally a submanifold h, such that the dynamics restricted to the center manifold for y sufficiently small, is given by the $(c = 2)$-dimensional vector field $\dot{y} = A_c y + F_c(y, h(y))$, $y \in \mathbb{R}^2$. Then, stability on the center manifold determines the stability of the fixed point. For k near k_{cr}, we can write

$$A_c = \begin{bmatrix} Re(\lambda(k)) & -Im(\lambda(k)) \\ Im(\lambda(k)) & Re(\lambda(k)) \end{bmatrix},$$

where $\lambda(k)$, $\bar{\lambda}(k)$ are the complex eigenvalues. The normal form then allows us to remove the quadratic nonlinearities and with $\lambda(k) \doteq \alpha(k) + i\omega(k)$ and by a Taylor expansion of these functions about k_{cr}, in polar coordinates the normal form is given by

$$\dot{r} = \alpha'(k_{cr})kr + a(k_{cr})r^3 + \mathcal{O}(k^2r, kr^3, r^5)$$
$$\dot{\theta} = \omega(k_{cr}) + b(k)r^2 + \mathcal{O}(r^4).$$

The coefficient $\alpha'(k_{cr})$ is simply the slope of the graph of the real part of the complex conjugate pair of eigenvalues and is easily seen to be negative in Figure 1.

Thus, there are two possible scenarios to this Hopf bifurcation. In the first, $a(k_{cr}) > 0$ in which case for $k > k_{cr}$ a repelling periodic orbit exists along with the stable fixed-point, and as k decreases below k_{cr}, the fixed point becomes unstable. In the second case, $a(k_{cr}) < 0$ and for $k > k_{cr}$ there is only a stable fixed point, while below k_{cr} a stable limit cycle exists along with the unstable fixed point. A routine computation verifies that $a(k_{cr}) < 0$, so that the transition from simple to chaotic dynamics must occur for $k < k_{cr}$.

We note that since $v_0 \mapsto Df(\bar{x})(v_0)$ is linear, the bifurcation point is independent of the choice of steady state velocity v_0. We also remark that the spectrum of Lyapunov exponents (which we discuss below) is a fairly reliable alternative to the computation of the normal form, for when stable limit cycles exist, the spectrum is $(0, -, -)$.

3 Remarks on various parameter ranges

For $k > k_{cr}$, the fixed point $\bar{x}$ defined in (4) is stable. By computing the divergence of the vector field f, we find the condition which makes it strictly negative:

$$\left(\frac{b_1}{a^2 L_1} + \frac{b_2}{a^2 L_2}, \frac{1}{aL_1} - \frac{b_1}{a^2 L_1} - \frac{b_2}{a^2 L_2}, \right.$$
$$\left. \frac{1}{aL_2} - \frac{b_1}{a^2 L_1} - \frac{b_2}{a^2 L_2} \right) \cdot (\tau, \theta_1, \theta_2)$$
$$< \frac{k}{a} + \frac{1}{L_1}\left(1 - \frac{b_1}{a}\right) + \frac{1}{L_2}\left(1 - \frac{b_2}{a}\right). \qquad (5)$$

The inequality (5) defines a plane of zero dissipation which divides the phase space into two regions, one of which contains the fixed point. In the region of space containing the fixed point, the dynamical system is dissipative and thus a volume element V is contracted by the flow into a volume element $V \exp^{\mathrm{div}f \, t}$ in a time t. The dissipative nature of the flow in this region implies that at least one eigenvalue of the linearized flow along the invariant set must have negative real part. If this were not the case, then near the invariant set, the flow would expand volume. For the same reason, the existence of invariant tori is precluded in this region of phase space.

For the parameters used herein (5) can be written in the simple form

$$4.16\tau - 0.16\theta_1 - 3.97\theta_2 - .01 < k, \qquad (6)$$

which translates into a constraint on the rate of slip of the block v, given by

$$v < e^{-3.15\theta_1 - 5.92\theta_2 + k}. \tag{7}$$

where these numbers are specific to the parameters we have considered. Equation (6) shows that the distance from the plane to $\bar{x}$ is a monotonically increasing function of k, and so as the spring is made stiffer, previously divergent trajectories now have the opportunity to converge to the steady state. Nevertheless, it is possible that trajectories may have initial rate of slip satisfying (7), but ultimately leave the region of phase space containing $\bar{x}$ and diverge. For example, this may occur if $\theta_1(0)$ and $\theta_2(0)$ are positive and large while $\tau(0)$ is small. Physically, this implies that the system starts with a very small slip rate compared to the steady state. In such a case, the rate of change of the internal state variables is initially very small thus keeping θ_1 and θ_2 almost constant. When k is small, the shear stress τ cannot increase at a fast enough rate to equilibrate the resisting forces of the internal state variables; therefore, the system has difficulty reaching the steady state as τ and θ_i slowly diverge. On the other hand, if the spring is very stiff, then the rate of change of the shear stress increases very quickly relative to the rate of change of the internal state variables, thus enabling the rate of slip to increase and ultimately attain the steady state.

An unfortunate artifact of the curve-fitting nature of this friction law, is that trajectories may violate the second law of thermodynamics. Since the rate of slip v is strictly positive, this will occur any time the shear stress τ is negative along the flow. (This actually occurs for flow along the limit cycles when $k < k_{cr}$.) As we have already mentioned, the shear stress is defined up to an additive reference stress τ^* and the velocity up to a multiplicative reference velocity v^*. The exact relationship is

$$\tau = \tau^* + \theta_1 + \theta_2 + a \log(\frac{v}{v^*}).$$

We have used $\tau^* = 0$ and $v^* = 1$, but it is clear that with the appropriate choice of τ^*, the region in which the dynamics are dissipative can be made "large". For this particular choice of reference parameters, we have numerically computed the basin of attraction of the fixed point $\bar{x}$ for various values of $k > k_{cr}$ and found bounded sets in each case, but the particular specification of the basin boundary is not of interest as it is simply for an arbitrary choice of τ^* and has no physical significance.

In the parameter range $k < k_{cr}$, numerical integration of the nonlinear system (3) confirms the bifurcation analysis. For k just below k_{cr}, limit cycles occur with period doubling bifurcations as k decreases (see Figure 2). When $k \sim .09075$, the attractor is no longer a periodic orbit, but rather contains an infinitude of them. This appears to be the onset of chaotic motion, and as a preliminary diagnostic, we compute the spectrum of Lyapunov exponents to quantify the attractor. This method has proven to be the most useful diagnostic of chaotic behavior. These exponents allow us to
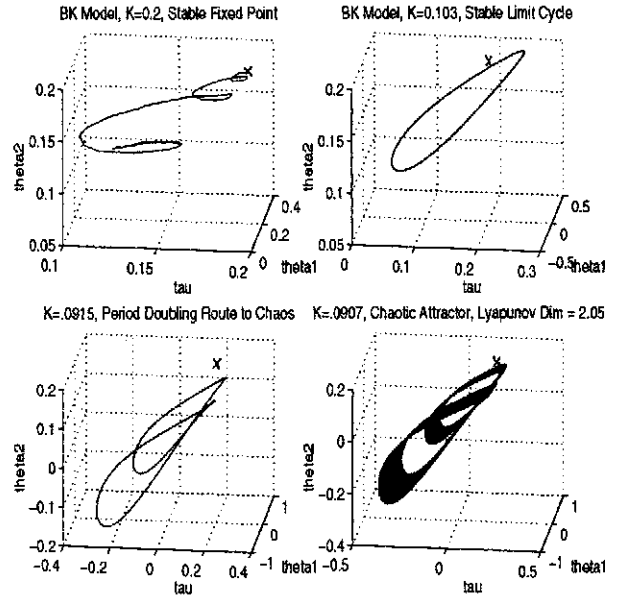

Fig. 2. Numerical integration reveals the period doubling route to chaotic dynamics as the stiffness parameter k is decreased.

study the geometry associated with the attraction and repulsion of orbits of (3) relative to $x(t)$ — exponential divergence of nearby orbits indicates a loss in predictive ability.

We consider trajectories $x(t)$ of (3) satisfying $x(0) = x_0$. Let $H \in C^\infty((0, \infty), gl(\mathbb{R}^3))$ (a smooth path in the general linear group of $\mathbb{R}^3$, i.e. the space of all 3x3 matrices) satisfying

$$\dot{H} = Df(x(t))H, \ H(0) = E$$

where E is some orthonormal frame. Then for any $v \in \mathbb{R}^3$ and with $\| \cdot \|$ the usual Euclidean norm, we can define the expansion associated with that direction along $x(t)$ as $\lambda_t(x_0, v) \equiv \|H(t)v\|/\|v\|$. Hence, the Lyapunov exponent corresponding to the trajectory $x(t)$ is defined as

$$\chi(x_0, v) \equiv \lim_{t \to \infty} \frac{1}{t} \log \lambda_t(x_0, v). \tag{8}$$

Since our phase space is not a compact manifold, and x_0 does not lie in a positively invariant set, (8) will only have meaning when the limit set itself is bounded. Our dynamical system will always have at least one zero exponent for $k < k_{cr}$ corresponding to the direction which is tangent to the flow; thus, in our three-dimensional phase space, the only possible spectra for values of k below k_{cr} are $(+, 0, -)$, a strange attractor or $(0, -, -)$, a limit cycle. It should be clear that an exponential expansion indicated by a positive Lyapunov exponent is incompatible with motion on a bounded attractor unless some sort of folding process merges widely separated trajectories.

For k in the interval $(.090755, k_{cr})$, we have computed a $(0, -, -)$ spectrum (see Figure 3), while for $k < .090755$, the spectrum contains a positive exponent indicating, in all likelihood, chaotic behavior. In particular, for $k = .0905$, the
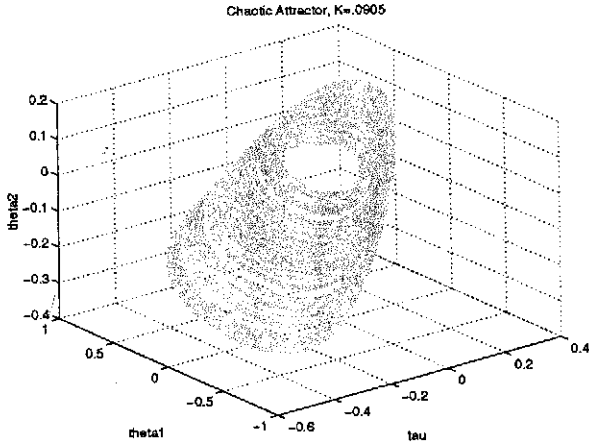
Fig. 3. The chaotic attractor at a stiffness $k = .0905$.

Fig. 4. Graphs of the family of unimodal map F_k for $k = .0907$, $.0906, .0905, .0904, .09036$ in increasing order from lowest to highest peak value. The mapping $k \to F_k(c)$ is monotonically decreasing where c is the critical point. For k small enough, $F_k(c) > 1$, and in this case, all of the interesting dynamics occur on some Cantor set.

exponents were found to be $(.025, 0, -.245)$ with a Lyapunov dimension $d_L = 2.1$, which is obtained by the following relations:

$$ d_L = j + \frac{\sum_{i=1}^{j} \chi(x_0, e_i)}{|\chi(x_0, e_{j+1})|}, $$

$$ \sum_{i=1}^{j} \chi(x_0, e_i) > 0, $$

$$ \sum_{i=1}^{j+1} \chi(x_0, e_i) < 0, $$

where e_i form the standard basis in $\mathbb{R}^3$.

4 Reduction to unimodal maps

In order to prove that the attractors are chaotic when $k < .09075$, we must show that the flow ϕ_t of (3) is sensitive to initial conditions, topologically transitive, and that periodic orbits are dense in the attractor. Since the chaotic attractor A_k (see Figure 3) graphically appears as though it lies on a Mobius strip, it should be possible to find a Poincaré section Σ in which the dynamics live on an invariant set that is a one dimensional manifold, i.e. $\Sigma \cap A_k$. We remark that although trajectories along A_k for $k < .09075$, comprise a geometrical shape resembling a Mobius strip, the attractor itself is not a Mobius strip as period doubling cannot occur on such a configuration manifold. In particular, the return map associated with a flow along the Mobius band cannot be unimodal.

As we are unable to solve for the actual invariant set analytically, we shall, in what follows, abuse terminology and use the term invariant set whenever the set is mapped within δ of itself, where δ refers to machine (single) precision. By this we mean that for a given fixed k, if P is the Poincaré map associated with the flow ϕ_t which maps the Poincaré section Σ back into Σ, then we shall call the set $\Sigma \cap A_k$ invariant if $dist(\Sigma \cap A_k, P(x)) < \delta$ for any $x \in \Sigma \cap A_k$. We also note that our computation of the invariant set requires interpolation between discrete data, and so we have made every
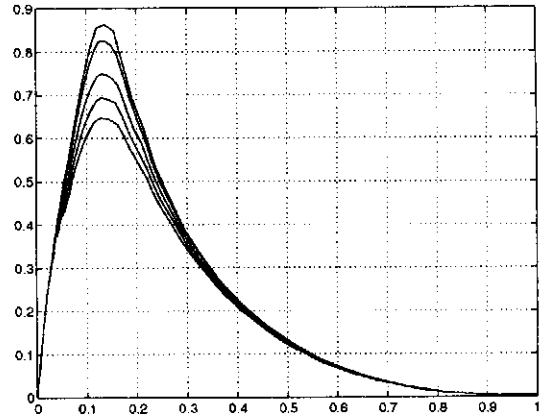
effort to be as precise as possible, using data points which are separated by $\mathcal{O}(\delta)$, and higher order polynomial interpolation. See Dahlquist (1974), for example, for efficient higher-order numerical schemes.

We choose our Poincaré section at $\theta_1 = .2$, and parameterize the invariant set of the Poincaré return map onto the unit interval I of the real line using arclength along the numerically computed one-dimensional manifold. This invariant set is the intersection of our Poincaré section with the attractor for the smallest value of k_{min} that we could numerically integrate. The invariance obviously only holds in some bounded interval of the stiffness parameter containing k_{min}, i.e. $\phi_{T(x)}(x, k) \in I$ for $x \in I$, $k \in (k_{min}, K] \subset (k_{min}, kcr)$, where $T(x)$ is the return time for x back to the Poincaré section Σ. Henceforth, whenever we refer to the return map, we shall mean the one dimensional mapping defined on the parameterized unit interval I.

Thus, as k varies in the interval $(k_{min}, K]$, we can numerically compute the one dimensional family of maps $F_k : I \to I$ on this interval I by tracking the first iterate of the Poincaré return map for initial conditions along the Poincaré section. Figure 4 shows that the family F_k is unimodal, and numerical computation gives us that F_k has negative Schwartzian derivative; hence, there is at most one attracting periodic orbit for each k in this range, and when k becomes small enough, no attracting periodic orbits exist. We note that points in the complement of I on the one dimensional manifold eventually diverge to $-\infty$ along the manifold under iteration of F_k.

The period doubling bifurcations which occur as k decreases can be seen by examining the graphs of the iterates F_k^n of F_k. Let p_k be the attracting fixed point for F_k when such a point exists and let $\hat{p}_k$ be its preimage under F_k. Then, the graph of F_k^2 on the interval $[\hat{p}_k, p_k]$ resembles the graph of F_k on I. Since we know that for $k < k_{cr}$, ϕ_t limits to

a periodic orbit, F_k must have an attracting fixed point for some range of k below k_{cr}. Hence, the first period doubling bifurcation occurs at the value of k where F_k^2 experiences a saddle node bifurcation on $[\hat{p}_k, p_k]$; the "hump" of F_k^2 grows until a period two point is born. This process is continued as k decreases until all the period 2^n points are born, and infinitely many periodic points with distinct periods exist.

In order to make this argument more precise, we simply need to show that F_k is a transition family. This means that there exists a k' for which the kneading sequence of $F_{k'}$ is $(000\bar{0}...)$, and a k'' for which the kneading sequence of $F_{k''}$ is $(100\bar{0}...)$, and that F_k has negative Schwartzian derivative for $k'' \leq k \leq k'$. It is clear from Figure 4 that the critical point c of F_k is independent of k and that $k \to F_k(c)$ is monotonically decreasing. Hence, we may choose k large enough so that $F_k(c) < c$ and let this value of k be k'. As for k'', we may choose a value just below .0903 for which $F_{k''}(c) = 1$. Graphical analysis confirms that $F_{k'}$ and $F_{k''}$ have the desired properties. As we noted, we numerically computed negative Schwartzian derivatives of F_k. This was done for about twenty distinct values of k and this leads us to conclude that the same must hold on the interval $[k'', k']$.

As k decreases, the transition family must become topologically conjugate to the shift map on the space of symbols representing the itinerary of the map F_k, and it is well known that the shift map is topologically transitive (see Devaney (1989) for a discussion and proof). Then, by topological conjugacy of the flow, the same qualitative behavior must occur in any section along the attractor.

We remark that although we used $v_0 = .5$ for our numerical studies, the vector field in (3) is structurally stable with respect to v_0, so that the same qualitative behavior persists in some parameter neighborhood. Finally, in order to relate this attractor to the physical phenomenon, we have displayed in Figure 5 the chaotic stick-slip motion along the attractor, by using the rate of slip v as one of the components of phase space. One can see that the slider sticks near zero velocity, then slips, and then sticks again.

5 Conclusions

We have combined geometric analysis with numerical experiments in an attempt to characterize the chaotic behavior of the nonlinear D-R slider in the smallest dimension which can exhibit such complexity, three. In particular, our analysis has confirmed the period doubling route to chaotic dynamics in the discretized D-R friction model with two internal state variables, and our reduction of the parameterized dynamics along the attractor to a family of unimodal maps suggest quite strongly that such chaotic dynamics persist in the temporally continous limit of zero time-step.

Nevertheless, the dynamics which we have examined are, in a sense, the "coarsest" possible, in that we only considered one slider as opposed to a continuum of sliders, and only two internal state variables as opposed to the spectrum of state variables needed to represent the true functional depen-
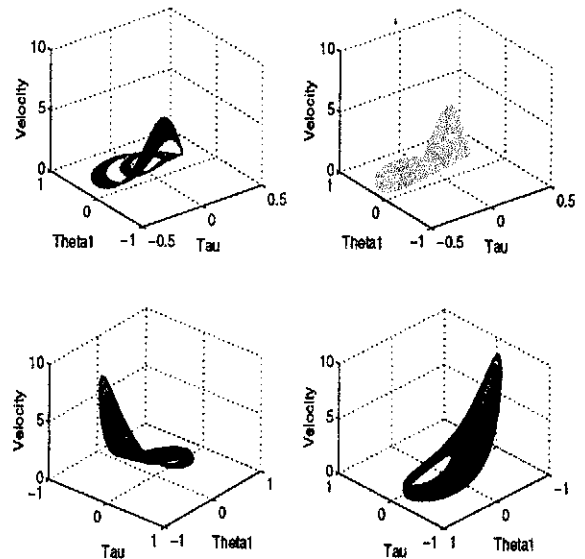

Fig. 5. Stick-slip chaotic motion displayed from various angles and with the stiffness parameter $k = .0907, .0905, .0904, .0903$ from top left going clockwise.

dence on velocity histories. Some thirty years ago, Burridge and Knopoff (1967) (see also Knopoff (1973)) proposed a landmark mathematical model to explore the role of friction along a fault as a factor in the earthquake mechanism, and their model consisted of a linear array of masses and springs representing a finite dimensional approximation to the continuum system. It is clear that as more and more sliders are added to the system, the model limits to a wave equation with highly nonlinear interface conditions modeling the friction. What remains unclear, however, is an appropriate continuum limit describing the frictional constitutive law along the interface, or fault.

The importance of having a rationally derived infinite dimensional dissipative model of frictional sliding cannot be overstated. First, infinite-dimensional dissipative nonlinear evolution equations possess universal finite-dimensional attractors, whose dimension can be estimated. Such an estimate would permit a sufficient level of discretization in order to capture numerically the evolution of the actual infinite-dimensional system. Second,for such dissipative nonlinear evolution laws it may be possible to constuct ordinary differential equations, called inertial manifolds, having the identical asymptotic behavior (see Jones and Shkoller (1997) for a detailed account of numerical approximation to attracting sets).

Our investigation of the simplest D-R model has been motivated by these considerations. In particular, the class of friction constitutive laws obtained by approximating the functional dependence of slip has on velocity history using a finite number of internal state variables, may serve as a sequence of finite-dimensional models from which we may infer the continuum limit. In this case, the finite-dimensional models must be robust enough to capture some of the complexities

observed in nature, and we have shown that the simplest D-R model does indeed meet this criterion.

References

M.L. BLANPIED, T.E. TULLIS, [1986], *The stability and behavior of a frictional system with a two state variable constitutive law*, Friction and Faulting, 124(3), 1986, 415-444.

R. BURRIDGE AND L. KNOPOFF, [1967], *Model and Theoretical Seismicity*, Bull. Seis. Soc. Amer., Vol. 57, No. 3, pp. 341-371.

J. CARR, [1981], *Applications of Center Manifold Theory*, Springer-Verlag.

G. DAHLQUIST, [1974], *Numerical Methods*, Prentice-Hall.

R.L. DEVANEY, [1989], *An Introduction to Chaotic Dynamical Systems*, 2nd. Ed., Addison-Wesley.

J.C. GU ET AL, [1984], *Slip motion and stability of a single degree of freedom elastic system with rate and state dependent friction*, J. Mech. Phys. Solids., 32, 167-196.

Y.J. GU AND WONG, T.F., [1991], *Effects of loading velocity, stiffness, and inertia on the dynamics of a single degree of freedom spring-slider system*, J. Geophys. Res., 96, B13:21677-21691.

Y. GU AND WONG, T.F., [1994], Nonlinear dynamics of the transition from stable sliding to cyclic stick-slip in rock, in *Nonlinear Dynamics and Predictability of Geophysical Phenomena*, edited by W.I. Newman, A. Gabrielov, and D.L. Turcotte, pp. 15-35, Am. Geophys. Union.

L. KNOPOFF ET AL, [1973], *The Dynamics of One-Dimensional Fault in the Presence of Friction*, Geophys. J.R. astr. Soc., Vol. 35, 169-184.

V.A. PLISS, G.R. SELL, [1991], *Perturbations of attractors of differential equations*, J. Differential Eq., **92**, 100-124.

A.L. RUINA, [1983], J. Geophys. Res., 88, No. B12, pp. 10359-10370.

D.A. JONES AND S. SHKOLLER, [1997], *Persistence of invariant manifolds for nonlinear PDEs*, to appear in Studies in Applied Mathematics, MIT.

J.D. WEEKS, [1993], *Constitutive laws for high-velocity frictional sliding and their influence on stress drop during unstable slip*, J. Geophys. Res., 98, No. B10:17637-17648.